Kaolin Valorisation as a Raw Material of Geopolymer Cement for Road Pavement Construction Used for Stabilizing Untreated Gravel

Khadhra ALLALI[1*], Nabil BELLA[1], Abderrahmane MEKKAOUI[1]

[1] FIMAS Laboratory, Faculty of Technology, Tahri Mohamed University Bechar Algeria
Corresponding author email: allali.khadra@univ-bechar.dz

Received: 11/01/2024 ; Accepted: 14/03/2024 ; Published: 24/03/2024

Abstract:

Road construction plays a vital role in a nation's development. However, increased traffic loads and road pavement degradation have led to the adoption of innovative materials, such as geopolymer cement (GPC), to address environmental concerns associated with conventional cement usage. GPC, produced through a chemical reaction involving alkali hydroxide, silicate, and aluminosilicate precursors, offers a solution to reduce carbon dioxide emissions and utilize low CO_2 emission technics. This study focuses on gravel treatment by alkali-activated metakaolin as the geopolymer precursor and activated with a mixture of sodium silicate and sodium hydroxide. Laboratory tests, including modified Proctor compaction, California Bearing Ratio (CBR), and unconfined compressive strength assessments, were performed with different NaOH dosages (8, 10, and 12 moles) in geopolymer-treated gravel. The results showed that geopolymer-treated gravel outperformed conventional cement-treated gravel, exhibiting higher dry density and unconfined compressive strength while meeting road foundation layer design standards. This research found that metakaolin-based geopolymer cement can substitut Portland cement in gravel treatment used in flexible pavement base layers, offering a sustainable alternative for road infrastructure development.

Keywords: -kaolin; alkali-activated materials; geopolymer cement; soil treatment; metakaolin based geopolymer; road base layer.

Tob Regul Sci.™ 2024; 10 (1): 1834 - 1861

DOI: doi.org/10.18001/TRS.10.1.116

1. Introduction

Road construction represents a fundamental component of a nation's development, playing a pivotal role in economic growth and transportation facilitation. The intricate pavement systems, comprising various layers such as surface asphalt, base, subbase, and the natural soil subgrade, efficiently distribute vertical forces generated by traffic and manage deformations [1]. According to the World Bank [2], global road spending in 2021 was estimated to be 2.3 Dollars trillion. This is expected to increase to 3.8 Dollars trillion by 2040, and the total length of paved roads in the world is estimated to be 60 million kilometres. Algeria has the third longest road network in Africa, with a total road network of 181,343 kilometres, of which 119,036 kilometres are paved. However, the escalating demands for accommodating heavy wheel loads and increasing traffic density have precipitated a reevaluation of road construction standards, necessitating superior materials like aggregates, bitumen, and various additives to elevate road performance [3]. These enhancements, while beneficial, have resulted in heightened construction, maintenance, and rehabilitation costs , thereby prompting an exploration of cost-effective and eco-friendly alternatives [4]. Traditionally, the construction industry has predominantly relied on cement and lime , with Ordinary Portland Cement (OPC) chemical stabilization being a global standard for enhancing soil and recycled materials in pavement base and subbase applications [5] [6] [7] [8] [9] [10] [11] [12] [13] [14]. Nevertheless, mounting concerns surround the environmental and economic implications of using OPC. The price of OPC has surged due to increasing energy costs, which has fueled the quest for affordable and readily available substitutes [15]. Furthermore, the production of OPC is accompanied by substantial greenhouse gas emissions, notably carbon dioxide (CO_2), contributing to global warming [16] [17]. The manufacture of 1000 kg of OPC clinker results in the direct emission of 550 kg of CO_2, with an additional 400 kg of CO_2 released through carbon-fuel combustion, bringing the total emissions from OPC production to a substantial 950 kg of CO_2 [18]. Consequently, there is an urgent need to explore alternative materials that are not only cost-effective but also environmentally sustainable, in order to ensure the continued development of road infrastructure. Alkali-activated materials, sometimes referred to as geopolymers, are emerging as promising alternatives with mechanical characteristics comparable to OPC [19] . In 1978, the term "geopolymer" was coined by the French scientist Joseph Davidovits to describe inorganic binders produced through alkaline activation of aluminosilicate precursors, resulting in a predominantly amorphous structure [20] . These aluminosilicate precursors, can be natural material as pouzzolane and metakaolin or industrial by-products like fly ash and slag, which are activated with an alkali silicate solution at

temperatures between 20°C and 100°C [12][21]. Geopolymers are known for their exceptional mechanical properties, chemical durability, and fire resistance, making them an environmentally friendly and durable material [22] [23]. Recent studies have demonstrated that geopolymers offer a viable alternative to OPC for reinforcing and enhancing degraded soils [24][25][26] [27], with several researchers reporting various applications of geopolymer cement in stabilized pavement base/subbase [28][29] [30] [31] [32] [33] [34] [35][36].

One of the most commonly used aluminosilicate precursors is Metakaolin (MK). MK obtained from calcined kaolin at temperatures between 650°C and 800°C, is an anhydrous aluminosilicate with good supplementary cementing properties [37]. Kaolin ($Al_4Si_4O_{10}$ $(OH)_8$) is a white aluminosilicate clay mineral, chemically inactive over a wide pH range, non-abrasive, non-toxic, dissolves easily in water, and has low heat and electricity conductivity [38] [39]. Kaolin, a versatile industrial mineral, is produced worldwide in excess of 25 million tonnes [40]. Some applications for kaolin include ceramics, pharmaceutical industries, paper coating, and fillers for paints and plastics [41]. Kaolin's application in fiberglass manufacture has grown considerably in the recent decade [42]. The most renowned and extensively utilized kaolin deposits are found in Cornwall, southwestern England, as well as in Georgia and South Carolina in the United States and the lower Amazon region of Brazil [43]. Africa also possesses numerous kaolin deposits used for various applications, including brick production, ceramics, fiberglass, plastics, pharmaceuticals, and more [44] . Algeria, for instance, has multiple kaolin deposits [Djebel Debbagh, Tamazert, Tabelbela …][45] [46]. Metakaolin-based geopolymers are created by combining concentrated alkaline hydroxide and silicate solutions with metakaolin powder [47]. These geopolymers exhibit unique properties, including early strength development, reduced thermal conductivity, improved acid resistance, and superior performance compared to conventional concrete [48]. Studies, such as Eisa et al. [30], have explored the use of metakaolin-based geopolymer concrete as a potential replacement for Portland cement concrete in rigid pavement slab applications. However, there have been relatively fewer studies focusing on metakaolin geopolymer for rigid pavements. Bella et al. [32] investigated the geotechnical characteristics of sand treated with metakaolin geopolymer cement for road base layers. However, there have been relatively fewer studies focusing on the use of metakaolin geopolymer for road construction. This scientific investigation explores the potential utilisation of metakaolin-based geopolymers as a substitute for traditional cementitious materials in the road base layer. The study follows a two-fold approach: firstly, the research encompasses the thermal treatment of kaolin, investigating the transformation into metakaolin through FTIR analysis to determine the

optimal temperature for the conversion process. Secondly, the study focus on a comprehensive set of laboratory assessments, including modified Proctor compaction, California Bearing Ratio, Unconfined Compressive Strength, and an investigation into the impact of varied NaOH dosages during the synthesis process of metakaolin-based geopolymers.

2. Materials And Methods

2.1. Materials

2.1.1. Kaolin

The kaolin used in this study was sourced from Makhlouf village, Tabelbala, Algeria. The Makhlouf kaolin deposit is situated within the municipal territory of Tabelbala and is geographically located at 29° 23' 20'' North and 03° 13' 50'' West (ORGM, 1985 and ORGM, 2000). This deposit is situated approximately 3 kilometers southeast of the commune headquarters and is referred to as the Makhlouf deposit due to its proximity to the village (Figure 1). In terms of its geological context, it is a part of the Kahal Tabelbala, the primary orographic feature of the Daoura beam. This deposit is found at the base of the Silurian formation on the southwest flank of the Kahal Tabelbala syncline, presenting itself as a prominent, visible hard bank spanning over 150 meters in length, with a thickness exceeding 10 meters, and exhibiting a dip of 10° to 30° towards the East (Figure 2). The kaolin within the deposit is characterized by its light gray to bluish coloration, oblique stratification, and the presence of hematite stringers. The deposit exhibits a low Quaternary cover. Moreover, a meteorological alteration zoning spanning a 3-meter slice is observed at the surface, gradually transitioning into pure kaolin as depth increases. Ksar Malhlouf kaolin deposit reserves were estimated at 500,000 tons (ORGM, 1984). kaolin's chemical composition was determined by X-ray fluorescent (XRF), and presented in table 1, the kaolin predominantly consists of silicon dioxide (SiO_2) and aluminum oxide (Al_2O_3), classifying it as a type of clay mineral.

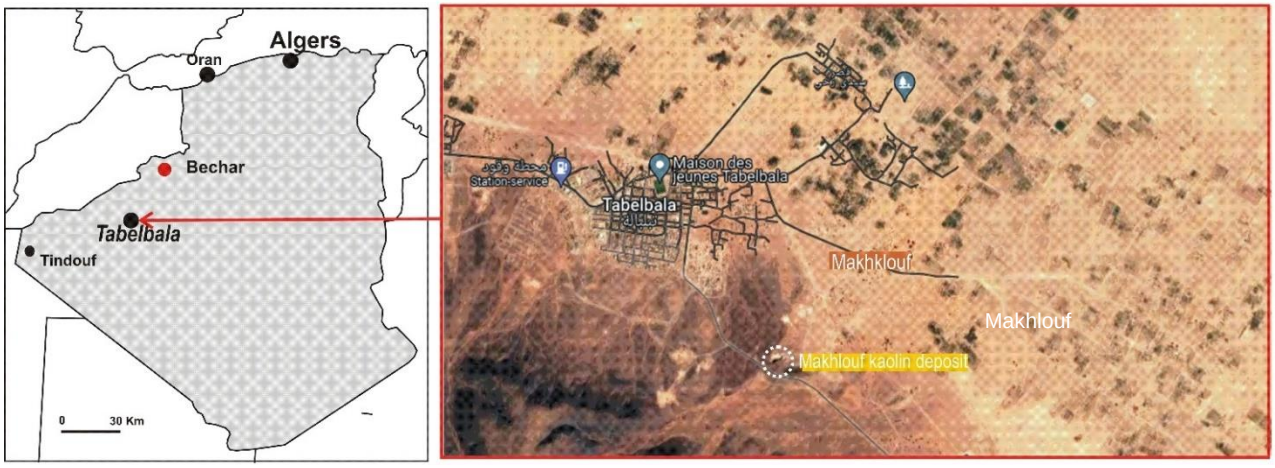

Fig. 1: Location of Makhlouf kaolin deposit

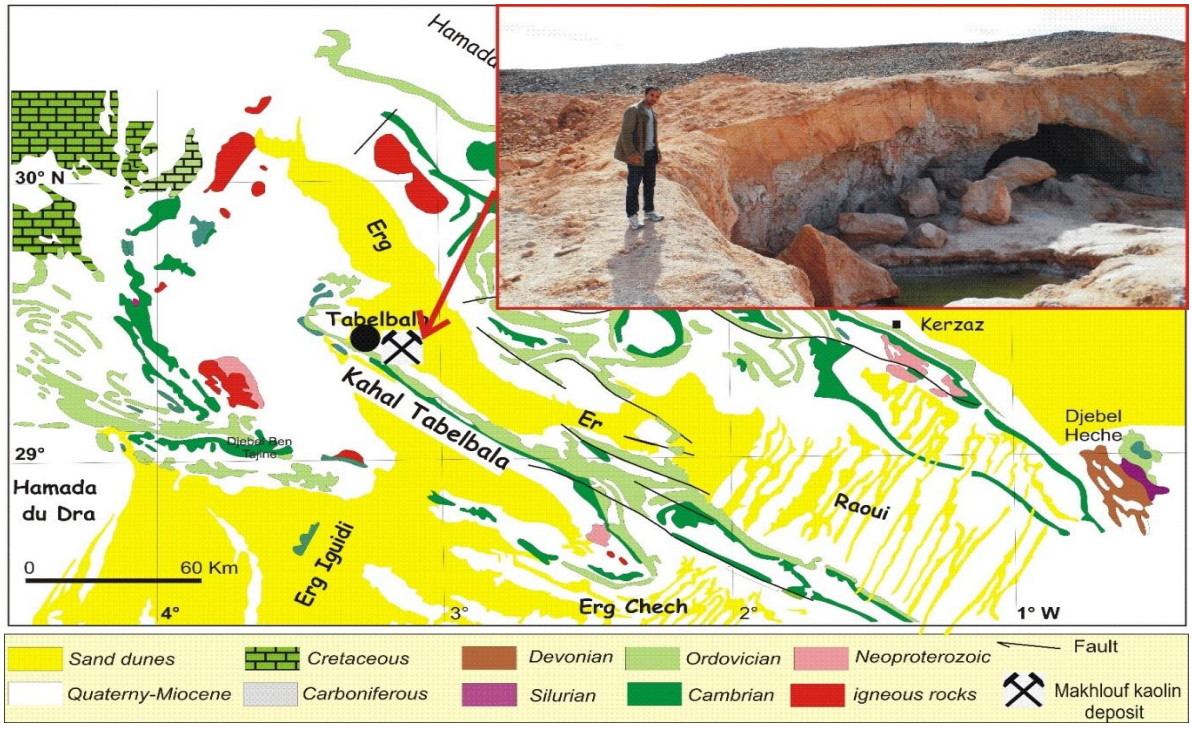

Fig. 2: Geological Sketch of the Kahal Tabelbala Region

Tab. 1: X-ray analyses of Kaolin

SiO_2	Al_2O_3	CO_2	Fe_2O_3	K_2O	TiO_2	SO_3	MgO	CaO	BaO	SrO	Other
52.99 %	31.88 %	4.9%	4.81%	2.13%	1.62%	0.92%	0.52%	0.41%	0.13%	0.07%	0.17%

Kaolin was milled using micro-grinder machine and we sift it through 125 µm sieve. The grain size distribution of kaolin was determined by Hydrometer analysis size distribution according to NF P 94-057, result shown in Figure 3.

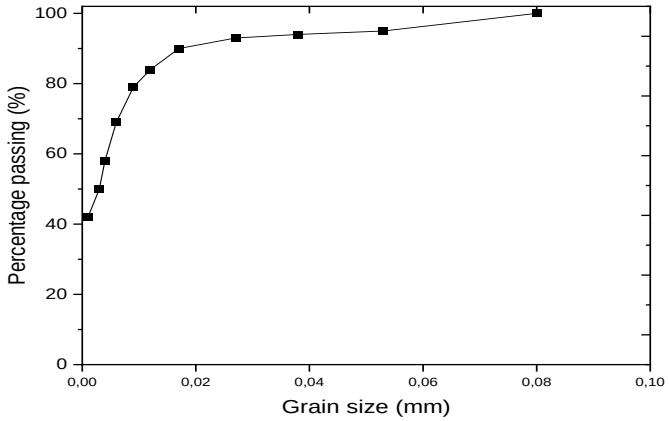

Fig. 3: Particle size distribution of Tabelbela Kaolin

2.1.2 Alkaline activator

The used alkaline activator was a solution of Water Glass and Sodium hydroxide. Water Glass (sodium hydroxide and water) was from SIGMA-ALDRICH, its formula is $Na2(SiO_2)$, xH_2O, with a density equal to 1,390, PH : 11,7. Sodium hydroxide was from commercial store its purity is 99%.The mixing water is taken from the drinking water of the city, it is from the "Djorftorba" dam 60 km from the town of Bechar.

2.1.3 Granulates

The used untreated gravel (UG) is the mixture of fine granulates (sand) granularity 0/3 (49%) and course granulates (gravel) granularity: 3/8 (19%), 8/15 (20%) and 15/25 (12%) from ELGHAZI YOUSSEF Company a crusher near Bechar mountain (Fig.4).

Fig. 4: Untreated Gravel aggregates

Figure 5 present the results of the grain size analysis by sieving the sand and gravel of the Djebel Bechar region according to NF P 94-056; the grain size curve of the untreated gravel fits into the spindle. According to the GTR 2000 Soil Classification [49] , The used untreated gravel belongs to the B5 class and is classified as gravelly soil with fines. Nait-Rabah et al.[50] found that if B5 soils are dry or moderately wet, compacting is very difficult. Thence, the UG need adding binders like cement or metakaolin geopolymer to improve their mechanical properties.

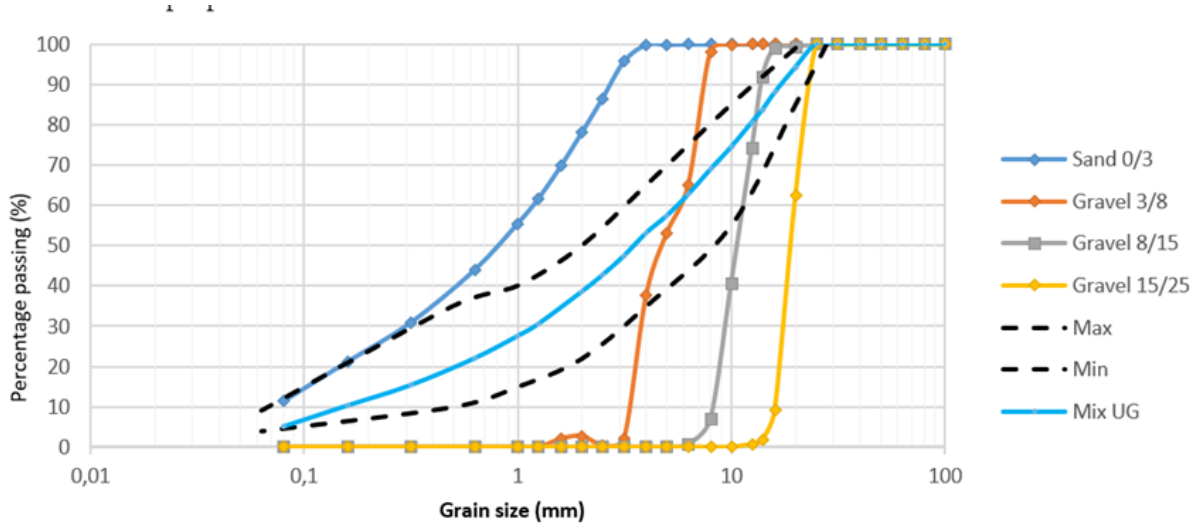

Fig. 5: Particle size distribution of UG 0/20

The physicochemical characteristics of Untreated Gravel (UG) as determined from the basic laboratory testing are summarised in Table 2.

Tab. 2: Physicochemical characteristics of UG

Geotechnical properties	Mean value	Test standards
Bulk density (g/cm^3)	2.32	NF EN 1936
Absolute density(g/cm^3)	2.63	//
methylene blue (MB)	0.4	NF EN 933-9
micro-Deval (MD)	17	NF EN-1097-1
Los Angeles (LA)	19	NF EN-1097-2
Sand equivalent (%)	74	NF EN 933-8
Carbonate $CaCO_3$ (%)	46.7	NF P 15-461
Sulfate SO_4^{-2}(%)	-	//

Chloride Cl- (%)	0.14	//
InsolublesSiO_2-MgO-AL_2O_3-CaO-Fe_2O(%)	53.16	//

2.1.4 Cement

In the conducted research, Portland cement (CEM II/A-L 42.5 N) from Saoura Cement Company (in Bechar) belonging to GICA (Algerian Cement Industrial Group) was utilized. This cement has a density of 3.06 g/cm³ and a specific surface of 3918 cm²/g. X-ray fluorescence (XRF) analysis was employed to determine the chemical properties of the cement, and the findings are documented in Table 3.

Tab. 3: XRF analyses of used cement

CaO	SiO_2	Al_2O_3	CO_2	Fe_2O_3	SO_3	MgO	K_2O	Sc_2O_3	TiO_2	SrO	Others
64.72 %	15.11 %	5.71 %	5.0%	3.75 %	3.07%	2.45%	0.82%	0.48%	0.19 %	0.04%	0.07 %

2.1.5 Mixes

The various mixtures, comprising treated gravel with cement and treated gravel with Metakaolin Geopolymer Cement (MKGPC) at different NaOH dosages (8, 10, and 12 moles), were studied as outlined in Table 4.

Tab. 4: Composition of treated Gravel with MKGPC

Compounds (g)	8 mol	10 mol	12 mol
Metakaolin (MK)	220	220	220
Water (total)	220	220	220
NaOH	46.48	64.08	81.68
WG (Water Glass)	174.88	174.88	174.88
W/MK	1	1	1
W_{WG}	110	110	110
W_{mix}	110	110	110

Gravel	**15/25**	633.6	633.6	633.6
	8/15	1056	1056	1056
	5/8	1003.2	1003.2	1003.2
	0/3	2587.2	2587.2	2587.2

2.2 Methods

First Kaolin heat treatment was studied using Fourier Transform Infra-Red (FTIR) spectroscopy, then modified Proctor compaction, California Bearing Ratio (CBR), and compressive strength tests were performed on untreated gravel (UG), Treated Gravel with Cement (TGC), and Treated Gravel with Geopolymer Cement (TGG).

2.2.1 Optimal temperature of Kaolin heat treatment

Kaolin was burned using Muffle furnace at different temperatures from 500°C to 700 °C during one hour, after that, Fourier Transformed Infra-Red (FTIR) analysis was done using the Cary 630 Agilent® FTIR Spectrometer with ATR sampling module machine to know the appropriate temperature to obtain Metakaolin.

2.2.2 Modified Proctor test

The compaction tests were carried out following the NF P94-093 Standard. The dry density ratio to moisture content is determined using compaction effort. It specifies the solid dry density and corresponding humidity, known as Optimal Moisture Content (OMC). Figure 7 illustrates the methodology used for the Modified Proctor test on the studied gravel. Mixtures in table 3 were compacted at different water content levels to determine the Optimum Moisture Content (OMC) and Maximum Dry Density (MDD) using the modified Proctor test.

Fig. 6: Modified Proctor test

2.2.3 California Bearing Ratio test (CBR)

The objective of this test is to assess the soil's ability to endure traffic loads and, consequently, ascertain the necessary thickness for pavement foundation layers. The process entails forming test specimens using the CBR mold, compacting them with 55 blows per layer, and adjusting their water contents to match the optimum moisture determined in the modified Proctor test. The CBR is then promptly determined after compaction following the standard procedure outlined in NF P94-078.

2.2.4 Unconfined compressive strength

In the current study, the mechanical properties of stabilised gravel are evaluated using the unconfined compressive strength test. In this test, cylindrical specimens of 100 mm diameter and 200 mm height were employed [51], and the specimen mould was plastic and removable. At first, the gravel specimens were prepared as Untreated Gravel (UG), Treated Gravel with Cement (TGC) and treated gravel with Metakaolin Geopolymer Cement with different dosages of NaOH (TGG 8moles, TGG 10moles and TGG 12moles). The values of maximum dry density,

optimum moisture content, cement content, metakaolin content and the alkaline activator content used for each specimen are shown in Table 5. For each test, three specimens were prepared and tested under the same conditions. Compacted samples were manufactured using the following method :

- The UG was dried in an oven.

- Gravel, cement, and metakaolin were weighed and mixed for approximately 10 minutes to yield a homogenous mixture.

- The gravel MK mix was homogenised by mixing an appropriate quantity of water (equivalent to the OMC) and the pre-prepared alkaline activator (water-NaOH and waterglass solution) for 15 min.

- Each specimen was filled with an appropriate quantity of the mixture and compacted into three layers (compact by 30 blows, using Modified Proctor rammer). After compaction, specimens were weighed when taken out of the mould.

- The specimens of UG and TGC were also prepared like the TGG specimens.

- The compacted specimens were covered in plastic film and stored in the curing room.

- The specimens (same optimal water content and maximum dry density) were cured for 1,7, 28 and 90 days before performing unconfined compressive strength tests under room temperature and constant humidity.

- The specimens that were cured and prepared for testing were removed from the curing chamber and storage, and the plastic coverings were removed. The specimens were then weighed to control the moisture variation.

- The unconfined compressive strength test was conducted according to the NF P 98-114-3, NF EN 13286-53, NF EN 13286-42, and NF EN 13286-41 Standard, and the compressive strength of the specimens was measured.

Tab. 5: Compaction characteristic of specimens

Specimens	Alkaline activator						Cement (%)	MK (%)	OMC (%)	MDD (g/cm3)
	Molar Concentrati	NaOH (g)	Waterglass	W_{WG}	W_{mix}	Water (tota				

	on		(g)	(g)	(g)	l) (g)				
UG	/	/	/	/	/	/	/	/	6	2.16
TGC	/	/	/	/	/	/	4	/	8	2.29
TGG	8moles	46.48	174.88	110	110	220	/	4	6.16	2.36
	10moles	64.08	174.88	110	110	220	/	4	6.16	2.39
	12moles	81.68	174.88	110	110	220	/	4	6.16	2.41

2.2.5 Microstructure analysis

Microstructure analysis of hardened geopolymer cement was done using FTIR previously described (in section 2.2), X Ray Diffraction (XRD) with a D8 Advance Eco diffractometer (Bruker®) operating with a copper tube (λ=1.54Å), and Scanning Electronic Microscopy (SEM) using Hitachi TM-1000 SEM (Hitachi, Tokyo, Japan) .

3. Results And Discussion

3.1 Optimal temperature of Kaolin heat treatment

The spectra of the FTIR analysis of kaolin and burned kaolin at several temperatures is shown in Figure 7. The FTIR peaks and corresponding functional groups are summarised in Table 6.

- Kaolin has the following stretching bonds, OH-Stretching of Hydroxyl group, Si=O, [Si/Al]-O stretching, OH-Deformation of hydroxyl group, and [Si/Al]-O.

- At 500 °C the kaolin keeps its properties in that all the bonds are almost the same.

- At 550 °C some of the OH-Stretching of the Hydroxyl group and Si=O groups disappeared as a result of the temperature effect which lead to kaolin transformation.

- At 600 °C a clear transformation for the kaolin happen, which is indicated by disappearing the groups of OH-Stretching of the Hydroxyl group, Si=O, [Si/Al]-O stretching, and OH-Deformation of the hydroxyl group.

- At 650 °C a threshold transformation for the kaolin appeared which was indicated by

disappearing a whole group of OH-Stretching of Hydroxyl group and most of Si=O, [Si/Al]-O stretching, OH Deformation of hydroxyl groups.

- At 700 °C the transformations already happened which indicates a resembles case for the heat treatment at 650 °C.

- From the mentioned information it can be determined that heat treatment for kaolin at 600 °C is the starting point for the transformation and the complete process happen at 650 °C.

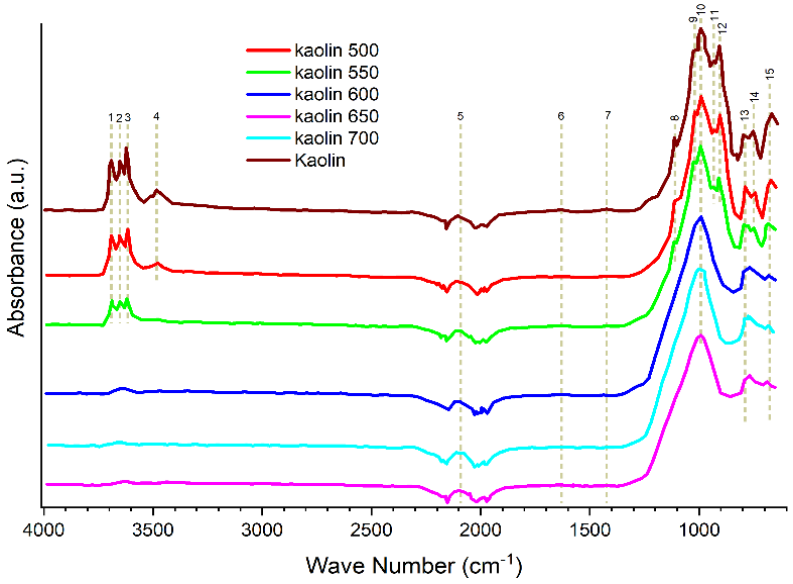

Fig. 7: FTIR spectra a) kaolin at R.T b) kaolin at 500°c c) kaolin at 550°c d) kaolin at 600°c e) kaolin at 650°c f) kaolin at 700°c

Tab. 6: The FTIR peaks and corresponding functional groups

Kaolin heat treated							
Description	700° C	650° C	600° C	550° C	500° C	R.T.	Peak No
OH-Stretching of Hydroxyl group				3687.58	3691.14	3691.42	1
			3652.025	3651.73	3655.26	3653.73	2
				3619.68	3615.58	3623.839	3
					3479.1	3483.2	4

					3		
Si=O	2076.098	2098.39	2120.244	2117.807	2112.52	2106.822	5
						1629.95	6
					1420.72	1422.74	7
[Si/Al]-O stretching				1104.241	1112.84	1113.1	8
				1025.48	1019.34	1025.88	9
	1000.243	990.53	990.98	992.89	990.53	992.0089	10
OH-Deformation of a hydroxyl group				932.055	932.9	931.58	11
				910.328	904.097	907.0532	12
[Si/Al]-O			796.61	795.175	789.39	798.032	13
	775.38	767.65	767.76	748.461	742.64	752.24	14
	683.91	688.83	681.19	683.82	670.34	667.2	15

3.2 Modified Proctor test

Figure 8 presents the results of the modified Proctor test conducted on the analyzed mixtures. For comparison, the maximum dry density of UG stands at 2.16 g/cm3, with an optimum moisture content of 6%. The treated Gravel with Cement (TGC) gave high maximum dry density than UG, estimated at 2.29 g/cm3, and the optimum moisture content is 8%. Gravel aggregates move closely, forcing fine aggregates (cement) to fill coarse aggregate voids. Thus, TGC compacts more than UG, increasing MDD [52]. TGGs with dosages of 8, 10, and 12 moles of NaOH showed a similar compaction curve with the same optimum moisture content of 6.16% (Take into consideration the water of alkaline activator). In the group of mixtures with variable dosage of NaOH, the maximum dry density value was 2.36 g/cm3 for blending with 8

moles of NaOH. The high dry density value in TGG compared to UT and TGC is significant, emphasising the stabilising effect of metakaolin geopolymer cement. The rise in dry density is attributed to the metakaolin geopolymer cement filling the pores in the UG material, resulting in a denser material. However, the moisture content sharply decreases in the treated gravel, demonstrating that geopolymer mixture activators work as lubricants to reduce repulsion forces and improve soil particle sliding [53]. Cement increases the water content in TGC. Cement fines absorb water, which enhances optimum water content and slightly lowers dry density [54]. The maximum dry density value is 2.41 g/cm3 (TGG 12mole), significantly higher than the obtained for the other tested group of mixtures. The TGC and the TGG had approximately 6% and 11% higher MDD than the UG, respectively. The TGG had an around 5% higher MDD than the TGC.

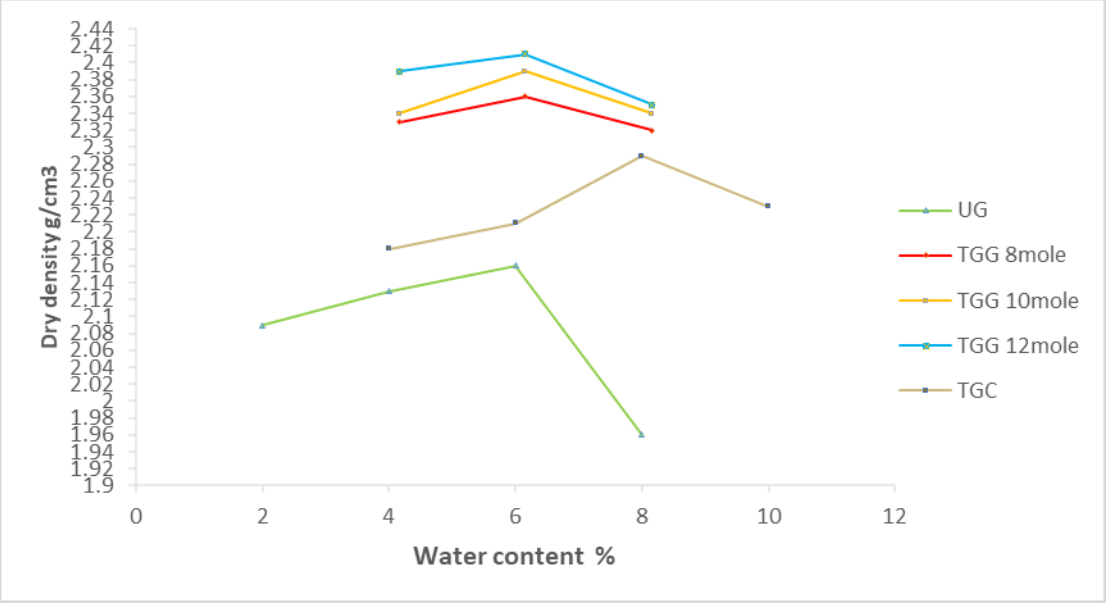

Fig. 8: Modified Proctor curve

3.3 California Bearing Ratio test

Figure 9 shows the histograms from the 95% Optimum moisture content CBR test on the mixtures. As a benchmark, UG exhibits a CBR of 107. In all cases, except for the TTG 12 moles, the CBR index values surpass 80%, which is the value mandated by the CEBTP stanrdard [55] for granular materials to be suitable as a base layer for flexible pavements. Upon analyzing Figure 14, it is evident that the highest CBR value was recorded in TGC, estimated at 125%, because of the stabilizing influence of cement, incorporating cement leads to a rise in CBR [56]. The CBR index exhibits a decline with increasing dosages of NaOH in the TGGs mixture, decreasing from

116% to 84% to 72% for TGG of 8, 10, and 12 moles, respectively. According to Zangana [57], All mixes treated with sodium hydroxide had a maximum CBR at an appropriate dosage and then decreased with increasing concentration. These results follow the opposite trend as the optimal dry densities of the Modified Proctor test (see Figure 8). A higher dry density usually results in a more compacted and denser material with less pore space and more particle interlocking. Thus, particle mobility and deformation under load may be restricted, lowering the CBR index.

Based on the CEBTP 1984 standard [55], the material must possess a CBR index higher than 80 (or 60 if low traffic). Both TGC and TGGs meet these requirements. However, further unconfined compression tests must be conducted to determine the appropriate dosage.

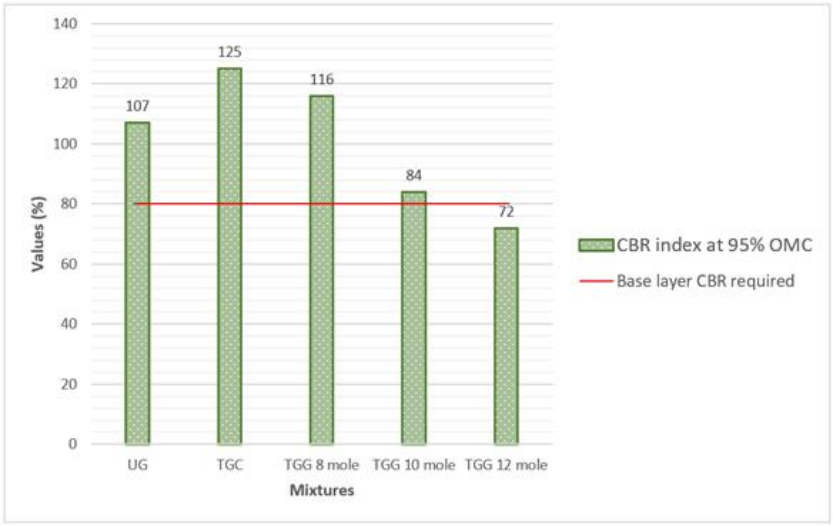

Fig. 9: Variation of the CBR index at 95% OPM of the mixtures

3.4 Unconfined compressive strength

Figure 10 shows the results of a unconfined compressive test. UG has an Unconfined Compressive Strength (UCS) as a reference value of 0, 0, 0.63 and 0.76 MPa for 1, 7, 28 and 90 days, respectively. All mixes show considerable UCS improvement. TGG8 have a maximum mean strength of 3.9 MPa (90 days). For TGC, UCS increases up to 2.83 MPa (28 days) and little bite decreases to 2.7 MPa (90 days). TGC has a substantially greater compressive strength than UG, which is normal because of cement hydration products formation. The results clearly show that the unconfined compressive strength of TGGs is greater than that of TGC approximately by 44% . The UCS of TGG8 raises for 1.21, 1.74, 2.71 and 3.9MPa for 1, 7, 28

and 90 days, respectively. In the case of TTG 10moles and TTG12, the UCS mesured 2.43, 3.23, 3.57 and 3.64 Mpa and 2.47, 3.04, 3.3 and 3.45 MPa for 1,7, 28 and 90 days, respectively. Thus, the TGG10 gave a UCS higher than TGG12, TGC and UG. The UCS of TGGs show a significant increase when compared to TGC and UG. The UCS of TGC samples increased slowly in the early age, and a decrease was observed on long term. The UCS of the TGG 10 and 12 moles samples rapidly increased in the early age and increased slowly over a long term (90 days), contrary to TGG8, which increases signifitically in long term by the rate of 44% compared to UCS at 28 days.

In general, unconfined compressive strength improved in all samples compared to untreated gravel. By the use of cement as UG treatment, unconfined compressive strength increases, even with a small amount of cement, compressive strength improves significantly [56].

The UCS of the TTG was very improved with increasing NaOH concentration from 8 to 10 and 12 moles in the early stages of 1,7 and 28 days. This is due to enhanced geopolymerisation output within the TTG due to the greater NaOH content, which increases pH [53]. In summary, the geopolymerization reaction process can be outlined as follows: Initially, the outer layer of metakaolinite particles dissolves in the NaOH solution, leading to the prompt polymerization of soluble aluminosilicate units in the presence of self-polymerizing species from the sodium silicate solution (including monomers, dimers, and larger oligomers with Si-O-Si chains). The resulting polymerized network then connects the dissolved metakaolinite particles. A higher concentration of NaOH solution dissolves metakaolinite particles more effectively and generates a polymerised network with a stronger link with the dissolved metakaolinite particulates [58].

According to Zhou et al. [59], in low-water conditions, increasing NaOH molarity strengthened stabilised soil. The growing concentration of OH^- ions accelerated the phase change of silicon and aluminium from their predecessors. However, a decrease in the UCS was noticed with a further increase in molarity beyond 8 moles. At 90 days of curing, the estimated UCS values were 3.57 MPa and 3.45 MPa for 10 and 12 moles, respectively. Excessive NaOH concentration may lead to depolymerization of the end product, resulting in a reduced quantity of binders [60].

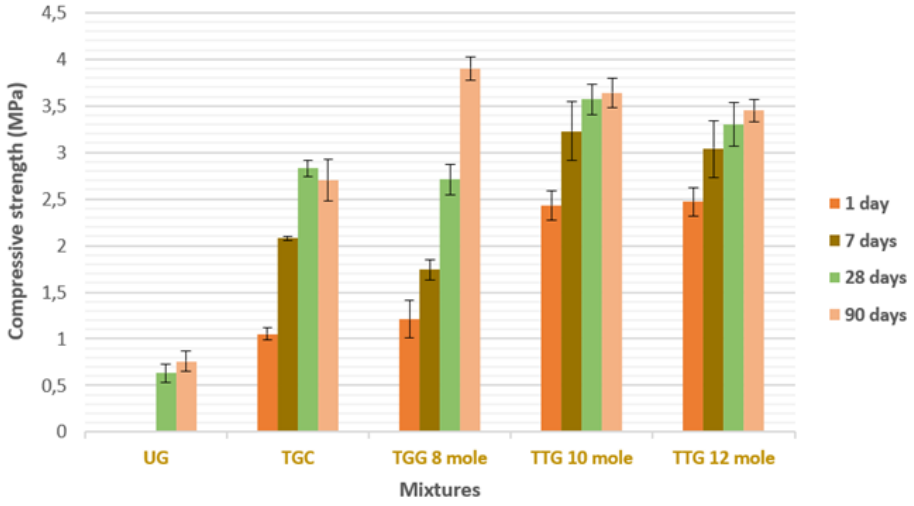

Fig. 10: Results of compressive strenght of untreated gravel and treated gravel mixtures.

3.5 Microstructure analysis

Figure 11 presents FTIR spectra of metakaolin burned under 650°C and metakaolin geopolymer hardened paste 28 days age of 8 moles NaOH. The FTIR peaks of GPMK 8moles and corresponding functional group are summarised in Table 7. This figure shows that in the geopolymer spectrum, the Si-O stretching vibration band may shift slightly, indicating the formation of a more polymerized Si-O network , the intensity of the Al-OH vibration band decreased in the geopolymer spectrum, suggesting the incorporation of aluminum into the geopolymer matrix groups, the appearance of a new band around 1420-1460 cm-1, which can be attributed to carbonate species from carbonation reactions in the geopolymer and The intensity and position of water-related peaks (around 3400 cm-1 and 1640 cm-1) changed, reflecting different states of water in the geopolymer matrix.

Figure 12 and 13 show the microstructure analysis (RDX , SEM) of metakaolin geopolymer hardened paste 28 days age of 8 moles NaOH. In RDX spectra, we note the presence of the following minerals: SiO_2 (PDF 87-2096), K(Al,Fe) $2AlSi_3O_{10}$ (OH) 2(PDF89-7536) and Fe_2O_3(PDF89-8104). In SEM image of GPMK 8moles, The geopolymer matrix shows varying degrees of porosity. The presence of small pores or voids is typical, resulting from the release of water during the geopolymerization reaction which leads to the formation of an amorphous to semi-crystalline aluminosilicate gel. This gel binds the unreacted particles together, often appears as a dense, homogeneous matrix encapsulating the particles. These results are consistent with those obtained by Zhou [59] , who attributed the decrease in UCS to the precipitation of $Ca(OH)_2$ owing to an elevated $\mathbf{OH^-}$ concentration.

According to Bilondi et al.[61], an optimal concentration of NaOH was necessary for proper geopolymerization and enhanced behavior of the geopolymeric specimens. Concentrations greater or lower than the optimal amount reduced the specimens' unconfined compressive strength. In the presented study, the concentration of NaOH of 8 moles was the appropriate dosage, which gave the high UCS. In comparing the UCS of TGC and TGGs, the TGG's UCS was higher than TGC's. The UCS and microstructure analysis results exhibited a similar trend as observed in the CBR tests. Therefore, we recommend utilizing the NaOH molarity of 8 moles to optimize benefits and cost-effectiveness in managing the mixes.

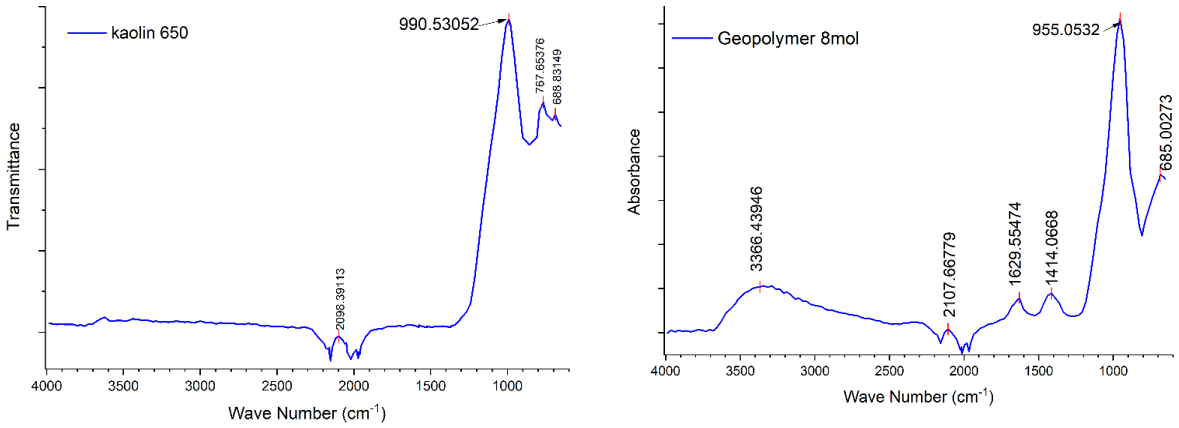

Fig. 11: FTIR Spectra of Metakaolin burned under 650°C and FTIR spectra of GPMK 8moles

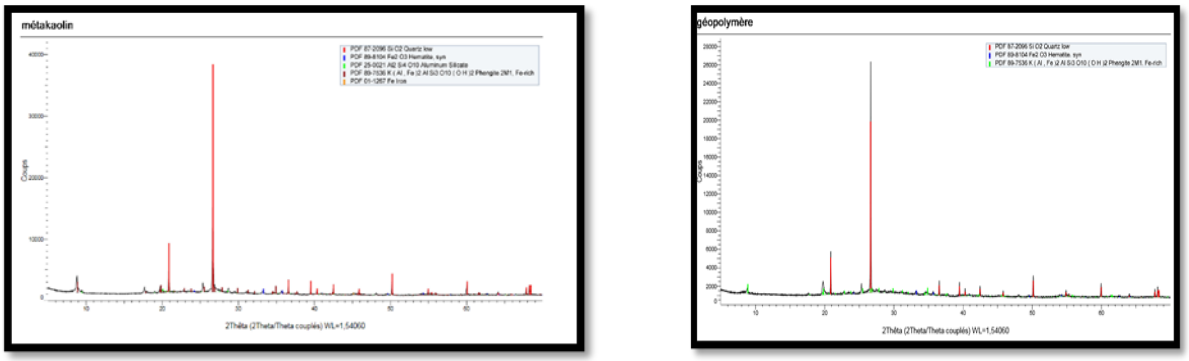

Fig. 12: RDX Spectra of Metakaolin burned under 650°C and FTIR spectra of GPMK 8moles

a)

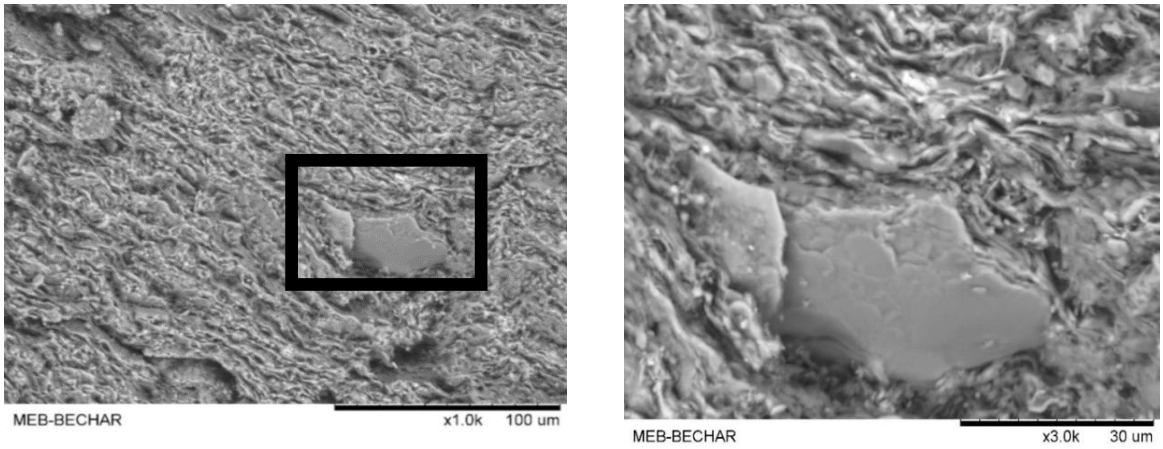

b)

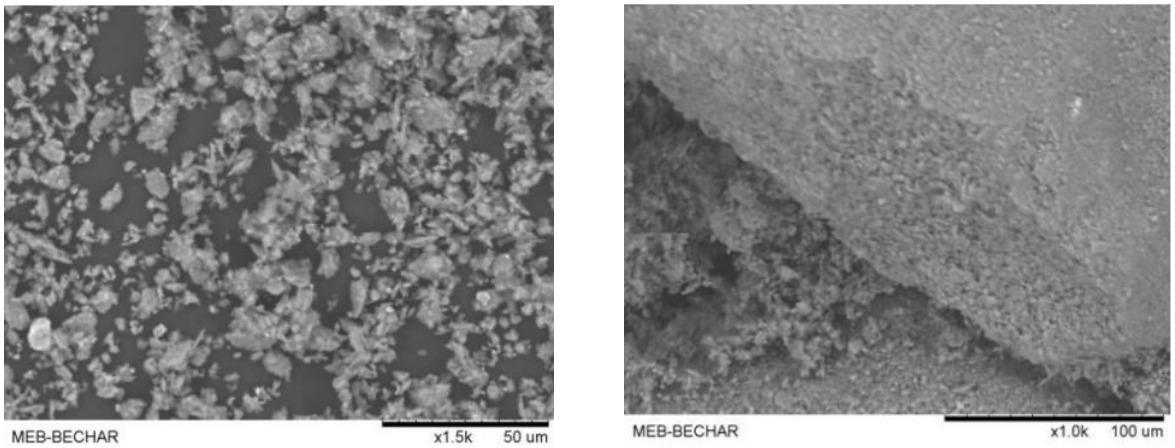

c)

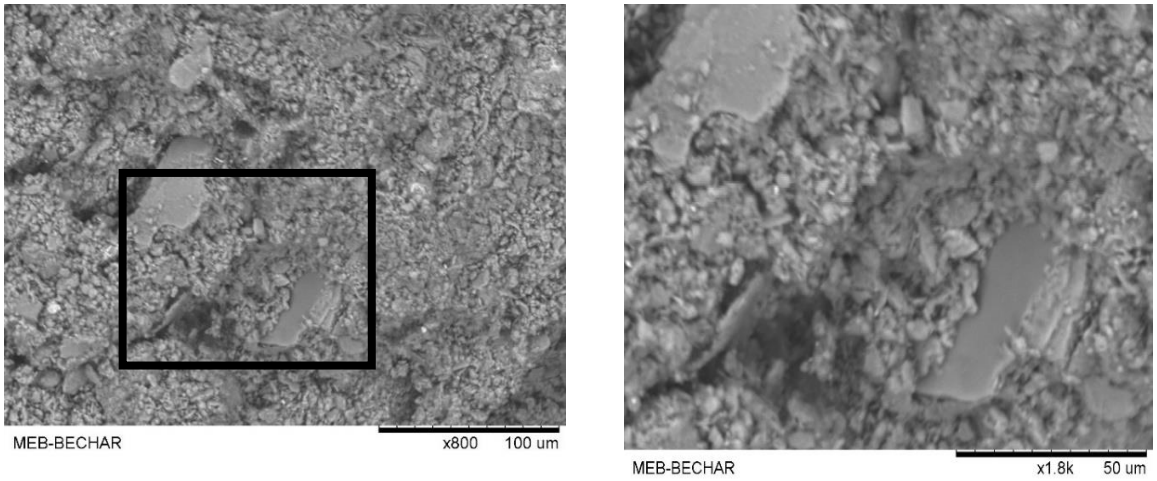

Fig. 13: SEM photo: a) kaolin , b) Metakaolin burned under 650°C and c) GPMK 8moles

Tab. 7: The FTIR peaks and corresponding functional groups

Peak No.	NaOH 8 moles	Description
1	3366,439	OH-Stretching
2	2107,6677	
3	1629,55	C-O
4	1414,066	OH
5	955,053	[Si/Al]-O stretching
6	685,002	[Si/Al]-O

4. Conclusions

In the construction of pavements, conventional stabilisers such as cement have been widely used to treat gravel, but they are significant contributors to global greenhouse gas eissions. Geopolymer cement is currently under investigation as a more sustainable alternative to conventional stabilizers for soil improvement. In the present study, a metakaolin-based geopolymer cement with varying doses of NaOH (8, 10, and 12 moles) was synthesised and used as the sole additive in untreated gravel compared to gravel treated with cement, and the following conclusions were reached:

- The FTIR analysis indicates that subjecting Kaolin to a thermal treatment at 650°C for one hour destroyed its crystalline structure, transforming it into an amorphous material known as metakaolin.

- Cement and Metakaolin possess pozzolanic properties that enhance mechanical characteristics. The metakaolin-based geopolymer cement enhances the mechanical properties.

- With the increase in NaOH dosages, there is a corresponding decrease in the optimum water content and an increase in the maximum dry density.

- The CBR values in Treated Gravel with Cement (TGC) were slightly greater than those obtained with the Treated Gravel with Geopolymer Cement (TGGs).

- The TGG's unconfined compressive strength (UCS)was higher than TGC's, and the concentration of NaOH of 8 moles was the appropriate dosage, which gave the high UCS.

- An optimal concentration of NaOH was essential for achieving appropriate geopolymerization and improved behavior of the geopolymeric specimens. Concentrations higher or lower than the optimal amount reduced the specimens' UCS.

- Finally, the optimal mixture was identified to enhance the properties of untreated gravel, making it suitable for application in pavement foundations. This mixture is TTG 8moles with dry density estimated at 2.36 g/cm3; CBR index = 116%, higher than 80% (the value required by the CEBTP for granular materials to be used as a base layer for flexible pavements) and a compressive strength approximately to 4MPa. Thus, we recommend using the NaOH molarity of 8 moles, which has the advantage of better performance and lower cost.

- Future research should focus on examining the performance of geopolymer cement with different Metakaolin ratios in stabilizing road base layers. This investigation should involve testing modified Proctor compaction, the California Bearing Ratio, and compressive strength to evaluate the effectiveness of the stabilization process.

Acknowledgement

The authors would like to thank the DGRSDT and ATRST for funding this research. Thanks also go to the LTPO laboratory, where almost all of these works were carried out, and Dahane Omar for FTIR analysis .

References

[1] Tom V. Mathew and K V Krishna Rao, ―Introduction to Transportation Engineering‖, NPTEL May 3, 2007

[2] World Bank, 1992. Rural Transport and the Village. World Bank, Washington, DC.

[3] V. Antunes, N. Simão, and A. C. Freire, "A Soil-Cement Formulation for Road Pavement Base and Sub Base Layers: a Case Study," *Transportation Infrastructure Geotechnology*, vol. 4, no. 4, pp. 126–141, 2017, doi: 10.1007/s40515-017-0043-9.

[4] A. J. Magalhães, G. J. C. Gomes, and P. J. M. Pires, "Toward improved performance of unpaved roads: laboratory tests and field investigation of a soil-byproduct base layer," *Road Materials and Pavement Design*, vol. 23, no. 1, pp. 184–198, 2022, doi: 10.1080/14680629.2020.1809503.

[5] M. M. Disfani, A. Arulrajah, H. Haghighi, A. Mohammadinia, and S. Horpibulsuk,

"Flexural beam fatigue strength evaluation of crushed brick as a supplementary material in cement stabilized recycled concrete aggregates," *Construction and Building Materials*, vol. 68, pp. 667–676, 2014, doi: 10.1016/j.conbuildmat.2014.07.007.

[6] A. Arulrajah, M. M. Disfani, H. Haghighi, A. Mohammadinia, and S. Horpibulsuk, "Modulus of rupture evaluation of cement stabilized recycled glass/recycled concrete aggregate blends," *Construction and Building Materials*, vol. 84, pp. 146–155, 2015, doi: 10.1016/j.conbuildmat.2015.03.048.

[7] Y. Hou, X. Ji, L. Zou, S. Liu, and X. Su, "Performance of cement-stabilised crushed brick aggregates in asphalt pavement base and subbase applications," *Road Materials and Pavement Design*, vol. 17, no. 1, pp. 120–135, 2016, doi: 10.1080/14680629.2015.1064466.

[8] X. Ji, Y. Jiang, and Y. Liu, "Evaluation of the mechanical behaviors of cement-stabilized cold recycled mixtures produced by vertical vibration compaction method," *Materials and Structures/Materiaux et Constructions*, vol. 49, no. 6, pp. 2257–2270, 2016, doi: 10.1617/s11527-015-0647-x.

[9] S. Caro, J. P. Agudelo, B. Caicedo, L. F. Orozco, F. Patiño, and N. Rodado, "Advanced characterisation of cement-stabilised lateritic soils to be used as road materials," *International Journal of Pavement Engineering*, vol. 20, no. 12, pp. 1425–1434, 2019, doi: 10.1080/10298436.2018.1430893.

[10] Y. Hou, X. Ji, and X. Su, "Mechanical properties and strength criteria of cement-stabilised recycled concrete aggregate," *International Journal of Pavement Engineering*, vol. 20, no. 3, pp. 339–348, 2019, doi: 10.1080/10298436.2017.1293266.

[11] D. R. Biswal, U. C. Sahoo, and S. R. Dash, "Non-destructive strength and stiffness evaluation of cement-stabilised granular lateritic soils," *Road Materials and Pavement Design*, vol. 21, no. 3, pp. 835–849, 2020, doi: 10.1080/14680629.2018.1511458.

[12] M. A. Gómez-Casero, F. J. Moral-Moral, L. Pérez-Villarejo, P. J. Sánchez-Soto, and D. Eliche-Quesada, "Synthesis of clay geopolymers using olive pomace fly ash as an alternative activator. Influence of the additional commercial alkaline activator used," *Journal of Materials Research and Technology*, vol. 12, pp. 1762–1776, 2021, doi: 10.1016/j.jmrt.2021.03.102.

[13] P. Chindaprasirt, P. Jamsawang, P. Sukontasukkul, P. Jongpradist, and S. Likitlersuang, "Comparative mechanical performances of cement-treated sand reinforced with fiber for road and pavement applications," *Transportation Geotechnics*, vol. 30, no. July, p. 100626, 2021, doi: 10.1016/j.trgeo.2021.100626.

[14] T. Yaowarat *et al.*, "Cement stabilisation of recycled concrete aggregate modified with polyvinyl alcohol," *International Journal of Pavement Engineering*, vol. 23, no. 2, pp. 349–357, 2022, doi: 10.1080/10298436.2020.1746311.

[15] G. M. Ayininuola and O. P. Oyedemi, "Impact of Hardwood and Softwood Ashes on Soil Geotechnical Properties," *Transnational Journal of Science and Technology (TSJT)*, vol. 3, no. 10, pp. 1–7, 2013.

[16] C. Teerawattanasuk and P. Voottipruex, "Comparison between cement and fly ash geopolymer for stabilized marginal lateritic soil as road material," *International Journal of Pavement Engineering*, vol. 20, no. 11, pp. 1264–1274, 2019, doi: 10.1080/10298436.2017.1402593.

[17] Joseph Davidovits, "Environmentally Driven Geopolymer Cement Applications," *Geopolymer 2002 Conference*, no. 6, pp. 1–9, 2002.

[18] T. Poltue, A. Suddeepong, S. Horpibulsuk, W. Samingthong, A. Arulrajah, and A. S. A. Rashid, "Strength development of recycled concrete aggregate stabilized with fly ash-rice husk ash based geopolymer as pavement base material," *Road Materials and Pavement Design*, vol. 21, no. 8, pp. 2344–2355, 2020, doi: 10.1080/14680629.2019.1593884.

[19] John L. Provis, "Alkali-activated materials," *Cement and Concrete Research*, vol. 114, pp. 40–48, 2017.

[20] J. Davidovits, "Geopolymers," *Journal of Thermal Analysis*, vol. 37, no. 8, pp. 1633–1656, 1991, doi: 10.1007/bf01912193.

[21] J. Temuujin, R. P. Williams, and A. van Riessen, "Effect of mechanical activation of fly ash on the properties of geopolymer cured at ambient temperature," *Journal of Materials Processing Technology*, vol. 209, no. 12–13, pp. 5276–5280, 2009, doi: 10.1016/j.jmatprotec.2009.03.016.

[22] H. S. Müller, M. Haist, and M. Vogel, "Assessment of the sustainability potential of concrete and concrete structures considering their environmental impact, performance and

lifetime," *Construction and Building Materials*, vol. 67, no. PART C, pp. 321–337, 2014, doi: 10.1016/j.conbuildmat.2014.01.039.

[23] J. Zhang, C. Shi, Z. Zhang, and Z. Ou, "Durability of alkali-activated materials in aggressive environments: A review on recent studies," *Construction and Building Materials*, vol. 152, pp. 598–613, 2017, doi: 10.1016/j.conbuildmat.2017.07.027.

[24] S. Wang, Q. Xue, W. Ma, K. Zhao, and Z. Wu, "Experimental study on mechanical properties of fiber-reinforced and geopolymer-stabilized clay soil," *Construction and Building Materials*, vol. 272, p. 121914, 2021, doi: 10.1016/j.conbuildmat.2020.121914.

[25] V. S. Jayawardane, V. Anggraini, A. T. Li-Shen, S. C. Paul, and S. Nimbalkar, "Strength Enhancement of Geotextile-Reinforced Fly-Ash-Based Geopolymer Stabilized Residual Soil," *International Journal of Geosynthetics and Ground Engineering*, vol. 6, no. 4, pp. 1–15, 2020, doi: 10.1007/s40891-020-00233-y.

[26] M. Syed, A. GuhaRay, S. Agarwal, and A. Kar, "Stabilization of Expansive Clays by Combined Effects of Geopolymerization and Fiber Reinforcement," *Journal of The Institution of Engineers (India): Series A*, vol. 101, no. 1, pp. 163–178, 2020, doi: 10.1007/s40030-019-00418-3.

[27] I. Chang, J. Im, and G. C. Cho, "Introduction of microbial biopolymers in soil treatment for future environmentally-friendly and sustainable geotechnical engineering," *Sustainability (Switzerland)*, vol. 8, no. 3, 2016, doi: 10.3390/su8030251.

[28] I. Phummiphan, S. Horpibulsuk, R. Rachan, A. Arulrajah, S. L. Shen, and P. Chindaprasirt, "High calcium fly ash geopolymer stabilized lateritic soil and granulated blast furnace slag blends as a pavement base material," *Journal of Hazardous Materials*, vol. 341, pp. 257–267, 2018, doi: 10.1016/j.jhazmat.2017.07.067.

[29] M. S. Eisa, M. E. Basiouny, and E. A. Fahmy, "Effect of metakaolin-based geopolymer concrete on the length of rigid pavement slabs," *Innovative Infrastructure Solutions*, vol. 6, no. 2, 2021, doi: 10.1007/s41062-021-00465-5.

[30] M. S. Eisa, E. A. Fahmy, and M. E. Basiouny, "Using metakaolin-based geopolymer concrete in concrete pavement slabs," *Innovative Infrastructure Solutions*, vol. 7, no. 1, 2022, doi: 10.1007/s41062-021-00601-1.

[31] J. Migunthanna, P. Rajeev, and J. Sanjayan, "Waste Clay Bricks as a Geopolymer Binder for

Pavement Construction," *Sustainability (Switzerland)*, vol. 14, no. 11, 2022, doi: 10.3390/su14116456.

[32] N. Bella, M. Boukar, K. Allali, F. Lemsadfa, and T. B. E. N. Moussa, "Eco-Cement based on Metakaolin Geopolymer , Used In Road Base Layer," vol. x.

[33] W. Hu *et al.*, "Mechanical property and microstructure characteristics of geopolymer stabilized aggregate base," *Construction and Building Materials*, vol. 191, pp. 1120–1127, 2018, doi: 10.1016/j.conbuildmat.2018.10.081.

[34] M. Hoy, S. Horpibulsuk, A. Arulrajah, and A. Mohajerani, "Strength and Microstructural Study of Recycled Asphalt Pavement: Slag Geopolymer as a Pavement Base Material," *Journal of Materials in Civil Engineering*, vol. 30, no. 8, 2018, doi: 10.1061/(asce)mt.1943-5533.0002393.

[35] D. Avirneni, P. R. T. Peddinti, and S. Saride, "Durability and long term performance of geopolymer stabilized reclaimed asphalt pavement base courses," *Construction and Building Materials*, vol. 121, pp. 198–209, 2016, doi: 10.1016/j.conbuildmat.2016.05.162.

[36] A. Mohammadinia, "Effect of geopolymer cement stabilisation on fatigue life of pavement sub-bases with recycled demolition aggregates," no. November, 2015.

[37] A. M. Rashad, "Metakaolin as cementitious material: History, scours, production and composition-A comprehensive overview," *Construction and Building Materials*, vol. 41, pp. 303–318, 2013, doi: 10.1016/j.conbuildmat.2012.12.001.

[38] K. Murugesh Babu, "Silk: Processing, properties and applications," *Silk: Processing, Properties and Applications*, vol. 6, pp. 1–264, 2018, doi: 10.1016/C2017-0-02174-2.

[39] V. Cantore, B. Pace, and R. Albrizio, "Kaolin-based particle film technology affects tomato physiology, yield and quality," *Environmental and Experimental Botany*, vol. 66, no. 2, pp. 279–288, 2009, doi: 10.1016/j.envexpbot.2009.03.008.

[40] C. Nkoumbou *et al.*, "Kaolin from Mayouom (Western Cameroon): Industrial suitability evaluation," *Applied Clay Science*, vol. 43, no. 1, pp. 118–124, 2009, doi: 10.1016/j.clay.2008.07.019.

[41] H. H. Murray, "Chapter 5 Kaolin Applications," *Developments in Clay Science*, vol. 2, no. C, pp. 85–109, 2006, doi: 10.1016/S1572-4352(06)02005-8.

[42] H. H. Murray, "Traditional and new applications for kaolin, smectite, and palygorskite: A general overview," *Applied Clay Science*, vol. 17, no. 5–6, pp. 207–221, 2000, doi: 10.1016/S0169-1317(00)00016-8.

[43] G. E. Christidis, "Industrial clays," *European Mineralogical Union Notes in Mineralogy*, vol. 9, no. 1, pp. 341–414, 2011, doi: 10.1180/EMU-notes.9.9.

[44] G. I. E. Ekosse, "Kaolin deposits and occurrences in Africa: Geology, mineralogy and utilization," *Applied Clay Science*, vol. 50, no. 2, pp. 212–236, 2010, doi: 10.1016/j.clay.2010.08.003.

[45] M. Taib, U. States, and G. Survey, "2014 Minerals Yearbook," no. November 2017, 2019.

[46] T. Rikioui, S. Lebaili, and A. Tafraoui, "Valorization of local kaolin in sustainable concrete and on the environment through their exploitation deposit," no. April, 2021, doi: 10.37789/rjce.2021.12.1.7.

[47] O. Ayeni, A. P. Onwualu, and E. Boakye, "Characterization and mechanical performance of metakaolin-based geopolymer for sustainable building applications," *Construction and Building Materials*, vol. 272, p. 121938, 2021, doi: 10.1016/j.conbuildmat.2020.121938.

[48] S. H. Mohmmad, P. Shakor, J. H. Muhammad, M. F. Hasan, and M. Karakouzian, "Sustainable Alternatives to Cement : Synthesizing Metakaolin-Based Geopolymer Concrete Using Nano-Silica," pp. 276–286, 2023.

[49] Gtr, "Réalisation des remblais et des couches de forme," p. 102, 2000.

[50] O. Nait-Rabah *et al.*, "Characterisation of Geotechnical Properties of Residual Tropical Soils Used for Road Infrastructure: French Guiana Experience," *Applied Sciences (Switzerland)*, vol. 13, no. 13, 2023, doi: 10.3390/app13137943.

[51] H. Gullu and K. Hazirbaba, "Cold Regions Science and Technology Uncon fi ned compressive strength and post-freeze – thaw behavior of fi ne-grained soils treated with geo fi ber and synthetic fl uid," vol. 62, pp. 142–150, 2010, doi: 10.1016/j.coldregions.2010.04.001.

[52] X. Ji, Y. Hou, X. Li, and T. Wang, "Comparison on properties of cement-stabilised gravel prepared by different laboratory compaction methods," *Road Materials and Pavement Design*, vol. 20, no. 4, pp. 991–1003, 2019, doi: 10.1080/14680629.2017.1423105.

[53] W. Hamid and A. Alnuaim, "Sustainable geopolymerization approach to stabilize sabkha soil," *Journal of Materials Research and Technology*, vol. 24, pp. 9030–9044, 2023, doi: 10.1016/j.jmrt.2023.05.149.

[54] H. G. R. Sekloka, C. P. Yabi, R. Cloots, and M. Gibigaye, "Elaboration of a Road Material Based on Clayey Soil and Crushed Sand," *Fluid Dynamics and Materials Processing*, vol. 18, no. 6, pp. 1596–1605, 2022, doi: 10.32604/fdmp.2022.022434.

[55] CEBTP, 1984. Practical guide to pavement design for tropical countries, 1984th ed. Experimental Center for Research and Studies in Building and Public Works, Paris, France.

[56] R. Pacheco-Torres and F. Varela, "Mechanical performance of cement-stabilised soil containing recycled glass as road base layer," *Road Materials and Pavement Design*, vol. 21, no. 8, pp. 2247–2263, 2020, doi: 10.1080/14680629.2019.1602073.

[57] D. Bahaadin Noory Zangana, "The Effect Of Sodium Hydroxide On The Strength Of Kirkuk Soil – Cement Mixtures," *Anbar Journal of Engineering Sciences*, vol. 5, no. 2, pp. 258–270, 2012, doi: 10.37649/aengs.2012.69038.

[58] H. Wang, H. Li, and F. Yan, "Synthesis and mechanical properties of metakaolinite-based geopolymer," *Colloids and Surfaces A: Physicochemical and Engineering Aspects*, vol. 268, no. 1–3, pp. 1–6, 2005, doi: 10.1016/j.colsurfa.2005.01.016.

[59] H. Zhou, X. Wang, Y. Wu, and X. Zhang, "Mechanical properties and micro-mechanisms of marine soft soil stabilized by different calcium content precursors based geopolymers," *Construction and Building Materials*, vol. 305, no. August, p. 124722, 2021, doi: 10.1016/j.conbuildmat.2021.124722.

[60]] Z. Yu *et al.*, "Microstructure and mechanical performance of alkali-activated tuff-based binders," *Cement and Concrete Composites*, vol. 139, no. December 2022, p. 105030, 2023, doi: 10.1016/j.cemconcomp.2023.105030.

[61] M. Pourabbas Bilondi, M. M. Toufigh, and V. Toufigh, "Experimental investigation of using a recycled glass powder-based geopolymer to improve the mechanical behavior of clay soils," *Construction and Building Materials*, vol. 170, pp. 302–313, 2018, doi: 10.1016/j.conbuildmat.2018.03.049.